Enhanced role of electron correlation in the hyperfine interactions in $^2D_{5/2}$ states in alkaline-earth-metal ions

B. K. Sahoo,[1,2,*] C. Sur,[2] T. Beier,[1] B. P. Das,[2] R. K. Chaudhuri,[2] and D. Mukherjee[3]

[1]*Atomphysik, GSI, Planckstraße 1, 64291 Darmstadt, Germany*

[2]*NAPP Group, Indian Institute of Astrophysics, Bangalore-34, India*

[3]*Department of Physical Chemistry, IACS, Kolkata-700 032, India*

The low-lying $n(=3,4,5)d$ $^2D_{5/2}$ states of alkaline-earth-metal ions are of vital importance in a number of different physical applications. The hyperfine structure constants of these states are characterized by unusually strong electron correlation effects. Relativistic coupled-cluster theory has been employed to carry out *ab initio* calculations of these constants. The role of the all-order core-polarization effects was found to be decisive in obtaining good agreement of our calculated magnetic dipole hyperfine structure constants with accurate measurements. The present work is an apt demonstration of the power of the coupled-cluster method to cope with strongly interacting configurations.

PACS number(s): 31.10.+z, 31.15.Ar, 31.15.Dv, 32.10.Fn

I. INTRODUCTION

The $^2S_{1/2} \rightarrow {}^2D_{5/2}$ transition frequencies in singly ionized alkaline-earth-metal atoms are among the leading candidates in the search for an optical frequency standard [1–3]. They are also of interest from the point of view of quantum information processing [4], parity nonconservation (PNC) arising from the nuclear anapole moment [5] and astrophysics [6]. A knowledge of the magnetic dipole hyperfine structure constant (A) for the $^2D_{5/2}$ states of these systems is essential for determining frequency standards [7]. Hyperfine interactions in these states are strongly influenced by electron correlation, and it is therefore of crucial importance to use a method that can treat accurately the strongly interacting configurations. The primary objective of this paper is to study the peculiar trends in the electron correlation in the hyperfine interaction constants for the $^2D_{5/2}$ states of the singly ionized alkaline-earth-metal atoms using the relativistic coupled-cluster (RCC) theory. This theory is equivalent to all-order many-body perturbation theory [8,9], and it has the potential to take into account the interplay of relativistic, and correlation effects. It has been successfully applied to understand the role of electron correlations in the studies of As in s and p valence systems [10–12] along with other important properties such as ionization potentials (IPs) [13,14], $E1$ transition amplitudes [15,16], and PNC [17]. However, the excited $^2D_{5/2}$ states of the alkaline-earth-metal ions are strongly affected by the core electrons [18]. Systematic investigations of the core-polarization (CP) effects in these systems can be carried out to obtain important insights into these phenomena.

II. THEORY

The magnetic dipole hyperfine constant A is given by [19,20]

$$A = \mu_N g_I \frac{\langle J \| \mathbf{O}^{(1)} \| J \rangle}{\sqrt{J(J+1)(2J+1)}}, \qquad (2.1)$$

where $\mathbf{O}^{(1)} = \Sigma_i o_q^{(1)}(r_i) = \Sigma_i - ie\sqrt{8\pi/3}\, r_i^{-2} \alpha \cdot \mathbf{Y}_{1q}^{(0)}(\hat{r}_i)$. The function $\mathbf{Y}_{kq}^{(\lambda)}$ represents a vector spherical harmonic, $g_I = \left[\frac{\mu_I}{I}\right]$ is the nuclear Landé g factor with μ_I being the nuclear dipole moment and $\mu_N = e\hbar/2m_p c$.

The electric quadrupole hyperfine constant (B) is given by [19,20]

$$B = 2eQ \left\{ \frac{2J(2J-1)}{(2J+1)(2J+2)(2J+3)} \right\}^{1/2} \langle J \| \mathbf{O}^{(2)} \| J \rangle, \qquad (2.2)$$

where Q is the nuclear quadrupole moment and $\mathbf{O}^{(2)} = \Sigma_i o_q^{(2)}(r_i) = \Sigma_i - e r_i^{-3} C_q^{(2)}(\hat{r}_i)$.

TABLE I. Total number of GTOs and active orbitals considered in the DF and RCC wave function calculations.

	$s_{1/2}$	$p_{1/2}$	$p_{3/2}$	$d_{3/2}$	$d_{5/2}$	$f_{5/2}$	$f_{7/2}$	$g_{7/2}$	$g_{9/2}$
Be⁺									
No. of GTOs	30	25	25	20	20	15	15	15	15
Active orbitals	12	11	11	11	11	7	7	5	5
Mg⁺									
No. of GTOs	30	25	25	20	20	15	15	15	15
Active orbitals	12	11	11	11	11	7	7	5	5
Ca⁺									
No. of GTOs	30	25	25	25	25	20	20	20	20
Active orbitals	13	12	12	12	12	7	7	5	5
Sr⁺									
No. of GTOs	35	30	30	25	25	20	20	20	20
Active orbitals	13	12	12	12	12	7	7	5	5
Ba⁺									
No. of GTOs	38	35	35	30	30	25	25	20	20
Active orbitals	13	13	13	13	13	9	9	8	8

*Electronic address: bijaya@mpipks-dresden.mpg.de. Present address: Max-Planck Institute for the Physics of Complex Systems, Dresden, Germany.

TABLE II. g_I values and Q values in b (=barn) used in the present work.

	Be	Mg	Ca	Sr	Ba
g_I	−0.78499	−0.34218	−0.37647	−0.243023	0.6249
Q	0.0529	0.199	−0.049	0.305	0.246

The matrix elements of the angular functions are given by

$$\langle \kappa_f m_f | C_q^{(k)} | \kappa_i m_i \rangle = (-1)^{j_f - m_f} \begin{pmatrix} j_f & k & j_i \\ -m_f & q & M_i \end{pmatrix} \langle \kappa_f \| C^{(k)} \| \kappa_i \rangle, \quad (2.3)$$

where $C_q^{(k)}$ is a component of the spherical tensor operator $\mathbf{C^{(k)}}$ [8] and i and f represent the initial and final single particle orbitals, respectively.

In the RCC theory, the atomic wave function $|\Psi_v\rangle$ for a single valence (v) open-shell system is given by [8,21]

$$|\Psi_v\rangle = e^T \{1 + S_v\} |\Phi_v\rangle, \quad (2.4)$$

where $|\Phi_v\rangle = a_v^\dagger |\Phi_0\rangle$, with $|\Phi_0\rangle$ being the Dirac-Fock (DF) state for the closed-shell system. The T and S_v are the closed-shell and open-shell excitation operators, respectively. In the single and double excitations approximation (CCSD) method, we have

$$T = T_1 + T_2 = \sum_{a,p} a_p^\dagger a_a t_a^p + \frac{1}{4} \sum_{ab,pq} a_p^\dagger a_q^\dagger a_b a_a t_{ab}^{pq}, \quad (2.5)$$

$$S_v = S_{1v} + S_{2v} = \sum_{p \neq v} a_p^\dagger a_v s_v^p + \frac{1}{2} \sum_{b,pq} a_p^\dagger a_q^\dagger a_b a_v s_{vb}^{pq}, \quad (2.6)$$

where $a^\dagger$ and a are the creation and annihilation operators, respectively. We have used $a, b, c, \ldots,$ and $p, q, r, \ldots,$ indices for the core and virtual orbitals, respectively. The amplitudes t_a^p and t_{ab}^{pq} are the corresponding single (T_1) and double (T_2) excitation operator amplitudes in the closed shell, and s_v^p and s_{vb}^{pq} are the cluster amplitudes for the single (S_{1v}) and double (S_{2v}) excitation operators involving the valence electron (v). Equations to determine these amplitudes with partial triple excitation effects [CCSD(T) method] are given elsewhere (for example, see Refs. [9,11]).
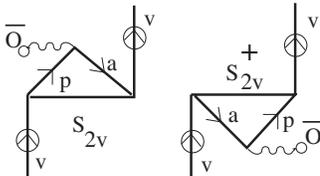

FIG. 1. Goldstone diagrams representing all-order CP effects from $\bar{O}S_{2v}$. Arrows pointing downwards and upwards represent core (a) and virtual (p) electrons, respectively. The arrow inside the circle represents valence electron.

III. METHOD OF CALCULATIONS

The hyperfine constants are determined in this theory by calculating the expectation value of the operator O as

$$\langle O \rangle_v = \frac{\langle \Psi_v | O | \Psi_v \rangle}{\langle \Psi_v | \Psi_v \rangle} = \frac{\langle \Phi_v | \{1 + S_v^\dagger\} e^{T^\dagger} O e^T \{1 + S_v\} | \Phi_v \rangle}{1 + N_v}$$

$$= \frac{\langle \Phi_v | \{1 + S_v^\dagger\} \bar{O} \{1 + S_v\} | \Phi_v \rangle}{1 + N_v}$$

$$= \frac{1}{1 + N_v} \{ \langle \Phi_0 | \bar{O} | \Phi_0 \rangle + 2\{\bar{O} S_{1v} + \bar{O} S_{2v}\}$$

$$+ S_{1v}^\dagger \bar{O} S_{1v} + S_{2v}^\dagger \bar{O} S_{1v} + S_{2v}^\dagger \bar{O} S_{2v} | \Phi_v \rangle \}, \quad (3.1)$$

where we define the effective operators $\bar{O} = e^{T^\dagger} O e^T$ and $N_v = \langle \Phi_v | S_v^\dagger e^{T^\dagger} e^T S_v | \Phi_v \rangle$. The above expression is calculated using the method described by [10,11]. Contributions from the normalization factor ($\mathcal{N}$) has been considered by

$$\mathcal{N} = \langle \Psi_v | O | \Psi_v \rangle \left\{ \frac{1}{1 + N_v} - 1 \right\}. \quad (3.2)$$

We use the Dirac-Coulomb (DC) atomic Hamiltonian for the CCSD(T) method in the present calculations. We employ Gaussian type orbitals (GTOs) to construct the DF wave function as explained in Ref. [22]. Finite nuclei with Fermi charge distribution are considered as given by Parpia and Mohanty [23]. Excitations from all the core-electrons have been allowed in both the DF and RCC calculations for all the systems.

IV. RESULTS AND DISCUSSIONS

In Table I, we present the total number of GTOs used for the DF, and active orbitals used for the RCC calculations in different systems. In Table II, we present the g_I and Q values

TABLE III. Dirac-Fock, all-order CP ($\bar{O}S_{2v}$+c.c.) and experimental results of the magnetic dipole hyperfine constant (A) of the $^2D_{5/2}$ states of the alkaline-earth-metal ions in MHz. Here c.c. is used to represent complex conjugate term.

	Be$^+$ $(3d_{5/2})$	Mg$^+$ $(3d_{5/2})$	Ca$^+$ $(3d_{5/2})$	Sr$^+$ $(4d_{5/2})$	Ba$^+$ $(5d_{5/2})$
DF	−1.020	−0.539	−14.163	−13.006	53.213
All order CP	0.057	0.659	15.793	18.795	−78.273
Expt.			−3.8(6)[a]	2.1743(14)[b]	−11.9(10)[c]
					−7.4(10)[d]
					−12.028(11)[e]

[a]Reference [26].
[b]Reference [27].
[c]Reference [28].
[d]Reference [29].
[e]Reference [30].

TABLE IV. CP contributions from single particle orbitals.

Core (a)	Virtual (p)	CP ($\bar{O}S_{2v}$)	Core (a)	Virtual (p)	CP ($\bar{O}S_{2v}$)
Be+					
$1s_{1/2}$	$2s_{1/2}$	0.0526	$1s_{1/2}$	$6s_{1/2}$	0.0028
$1s_{1/2}$	$3s_{1/2}$	0.0004	$1s_{1/2}$	$8s_{1/2}$	−0.0008
$1s_{1/2}$	$4s_{1/2}$	0.0004	$1s_{1/2}$	$7d_{3/2}$	0.0004
Mg+					
$1s_{1/2}$	$8s_{1/2}$	−0.0056	$2s_{1/2}$	$9s_{1/2}$	0.0192
$1s_{1/2}$	$9s_{1/2}$	−0.0097	$2p_{1/2}$	$3p_{1/2}$	−0.0242
$2s_{1/2}$	$3s_{1/2}$	0.2591	$2p_{1/2}$	$7p_{1/2}$	−0.0183
$2s_{1/2}$	$4s_{1/2}$	0.0240	$2p_{1/2}$	$8p_{1/2}$	−0.0147
$2s_{1/2}$	$5s_{1/2}$	0.0097	$2p_{3/2}$	$3p_{3/2}$	0.1680
$2s_{1/2}$	$6s_{1/2}$	0.0135	$2p_{3/2}$	$4p_{3/2}$	0.0136
$2s_{1/2}$	$7s_{1/2}$	0.0903	$2p_{3/2}$	$6p_{3/2}$	0.0114
$2s_{1/2}$	$8s_{1/2}$	0.0861	$2p_{3/2}$	$7p_{3/2}$	0.0498
Ca+					
$2s_{1/2}$	$8s_{1/2}$	0.6576	$2p_{1/2}$	$9p_{1/2}$	−0.3196
$2s_{1/2}$	$9s_{1/2}$	1.6782	$3p_{1/2}$	$8p_{1/2}$	−0.2283
$2s_{1/2}$	$10s_{1/2}$	0.8119	$3p_{1/2}$	$9p_{1/2}$	−0.5072
$3s_{1/2}$	$4s_{1/2}$	2.0285	$3p_{3/2}$	$4p_{3/2}$	0.7231
$3s_{1/2}$	$7s_{1/2}$	0.8361	$3p_{3/2}$	$7p_{3/2}$	0.4276
$3s_{1/2}$	$8s_{1/2}$	3.1017	$3p_{3/2}$	$8p_{3/2}$	0.9689
$3s_{1/2}$	$9s_{1/2}$	2.8690	$3p_{3/2}$	$9p_{3/2}$	0.8745
Sr+					
$2s_{1/2}$	$11s_{1/2}$	0.8428	$4p_{1/2}$	$9p_{1/2}$	−0.9871
$4s_{1/2}$	$5s_{1/2}$	4.4052	$4p_{1/2}$	$5p_{3/2}$	1.2774
$4s_{1/2}$	$6s_{1/2}$	0.9198	$4p_{3/2}$	$8p_{3/2}$	0.9915
$4s_{1/2}$	$8s_{1/2}$	2.3399	$4p_{3/2}$	$9p_{3/2}$	2.1803
$4s_{1/2}$	$9s_{1/2}$	6.6872	$4p_{3/2}$	$10p_{3/2}$	0.7558
$4s_{1/2}$	$10s_{1/2}$	−0.8056	$3d_{5/2}$	$10d_{5/2}$	−0.4921
Ba+					
$2s_{1/2}$	$12s_{1/2}$	−1.9393	$5p_{1/2}$	$9p_{1/2}$	2.2198
$4s_{1/2}$	$10s_{1/2}$	2.2430	$5p_{1/2}$	$10p_{1/2}$	4.6907
$4s_{1/2}$	$11s_{1/2}$	−1.8759	$3p_{3/2}$	$13p_{1/2}$	−1.0486
$5s_{1/2}$	$6s_{1/2}$	−20.5902	$4p_{3/2}$	$10p_{1/2}$	1.5367
$5s_{1/2}$	$7s_{1/2}$	−4.5075	$5p_{3/2}$	$6p_{3/2}$	−4.3027
$5s_{1/2}$	$8s_{1/2}$	−1.5996	$5p_{3/2}$	$7p_{1/2}$	−1.1738
$5s_{1/2}$	$9s_{1/2}$	−16.6304	$5p_{3/2}$	$9p_{3/2}$	−5.9189
$5s_{1/2}$	$10s_{1/2}$	−28.6553	$5p_{3/2}$	$10p_{3/2}$	−8.7231
$2p_{1/2}$	$12p_{1/2}$	1.0509	$4d_{5/2}$	$10d_{5/2}$	1.7734
$5p_{1/2}$	$7p_{1/2}$	1.2755	$4d_{5/2}$	$11d_{5/2}$	1.9755

FIG. 2. (Color online) Core-polarization contributions to A/g_I (MHz) for different systems.

constants in the considered systems, we present the DF and $\bar{O}S_{2v}$ contributions along with the experimental results of A for different states in Table III. It is obvious from this table that the DF and the measured values have opposite signs except for Ca+. The contributions from $\bar{O}S_{2v}$ are larger than the DF values for all the ions except Be+, which has only one core orbital. Their inclusion significantly improves the agreement of A with the experimental values for all the ions.

A deeper understanding of these results can be obtained from Table IV, where we have given the all-order CP contribution to A from different core (a) and virtual (p) orbitals. It is clear from this table that the valence or the low-lying continuum orbitals, and the outer core orbitals contribute more than the other orbitals. The significant contributions due to the valence orbitals arise from the large size of the hyperfine matrix elements, and the small energy differences involving the valence and the outer core orbitals. Even

TABLE V. The magnetic dipole hyperfine structure constants (A) in MHz.

System	State	This work		Others		Experiment	
^{9}Be+	$3d\ ^2D_{5/2}$	−0.0	976				
^{25}Mg+	$3d\ ^2D_{5/2}$	0.0	107	0.0	1196[a]		
^{43}Ca+	$3d\ ^2D_{5/2}$	−3.0	351	−5.0	2[b]	−3.0	8(6)
				−4.0	2[c]		
				−3.0	552[d]		
				−4.0	84[e]		
^{87}Sr+	$4d\ ^2D_{5/2}$	2.0	156	1.0	1[f]	2.0	1743(14)
				2.0	507[d]		
				−2.0	77[e]		
^{137}Ba+	$5d\ ^2D_{5/2}$	−11.0	717	9.0	39[e]	−12.0	0.28(11)

[a]Reference [31].
[b]Reference [32].
[c]Reference [33].
[d]Reference [34].
[e]Reference [35].
[f]Reference [36].

that are used to calculate A and B, respectively, for various systems [24,25].

The terms involving OS_{2v} in the expansion of Eq. (3.1) represent the all-order CP effect [10]. The dressing of the hyperfine interaction by the core is reflected through the effective operator $\bar{O}$. Therefore, one could consider $\bar{O}S_{2v}$ as an all-order CP effect, and the diagrams associated with them are given in Fig. 1. In order to highlight the spectacular role of the CP effects in the magnetic dipole hyperfine structure
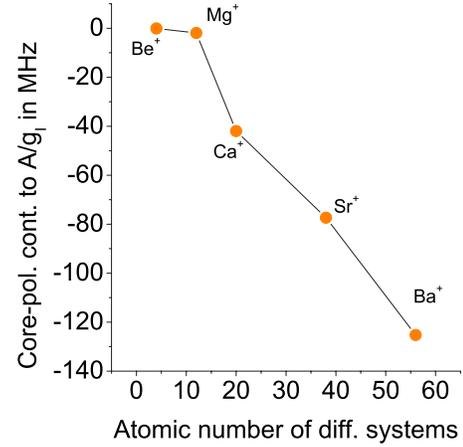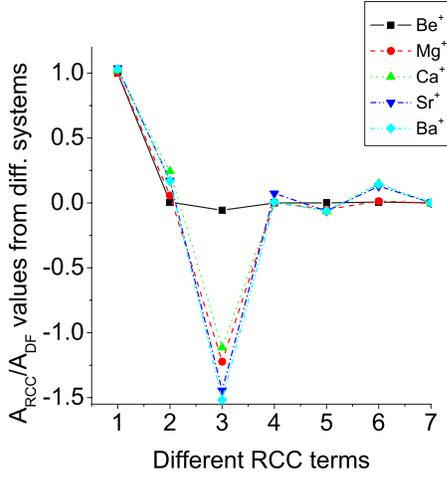
FIG. 3. (Color online) $A_{\text{RCC}}/A_{\text{DF}}$ values for different systems for the RCC terms arising from Eq. (3.1). In the X axis, $\bar{O}$, $\bar{O}S_{1v}$+c.c., $\bar{O}S_{2v}$+c.c., $S_{1v}^{\dagger}\bar{O}S_{1v}$, $S_{2v}^{\dagger}\bar{O}S_{1v}$+c.c., $S_{2v}^{\dagger}\bar{O}S_{2v}$, and normalization terms are taken in a sequence in each unit distance.

TABLE VII. The electric quadrupole hyperfine structure constants (B) in MHz.

System	State	Others	This work	Experiment
^{9}Be^{+}	3d $^{2}D_{5/2}$		0.119	
^{25}Mg^{+}	3d $^{2}D_{5/2}$		1.743	
^{43}Ca^{+}	3d $^{2}D_{5/2}$	−4.462[a] −4.4[c]	−4.310	−3.9(6.0)[b]
^{87}Sr^{+}	4d $^{2}D_{5/2}$	54.4[c] 53.6[e]	49.166	49.11(6)[d]
^{137}Ba^{+}	5d $^{2}D_{5/2}$	61.12[f]	62.179	62.5(50)[g] 60.7(10)[h] 59.533(43)[i]

[a]Reference [31].
[b]Reference [37].
[c]Reference [34].
[d]Reference [27].
[e]Reference [36].
[f]Reference [35].
[g]Reference [28].
[h]Reference [29].
[i]Reference [30].

though the high-lying (s and p) continuum orbitals have large densities at the nucleus, their contributions are small. Their energies are rather large compared to the core orbitals, and this makes their contributions to A almost insignificant. Since the energies of orbitals higher than the g symmetries are larger than the most important contributing continuum orbitals, their contributions in the present calculations are expected to be very small and hence they have been neglected here.

From Eq. (2.1), it is clear that A depends on both the nuclear Landé g factor (g_I) and the matrix elements of the hyperfine interaction operator, which depends on the single particle wave functions in the nuclear region. It would, therefore, be appropriate to study the variation in electron correlation in different systems by examining the results of A/g_I.

The CP effects arising from different systems for the low-lying $^{2}D_{5/2}$ states are presented in Fig. 2 by plotting the ratio of the contributions of $\bar{O}S_{2v}$ with the corresponding g_I. These contributions have negative signs, and they are very pro-

nounced in heavier systems. It is more than 100% in the case of Ba^{+}.

In Table V, we give the results of our RCC calculations for the final values of A as well as those of other calculations and measurements wherever available. In order to appreciate the relative importance of the different physical effects, we plot the fractional contributions of various RCC terms with respect to DF values for the corresponding states in Fig. 3 and actual contributions are given in Table VI for all the ions. As shown in this figure, contributions from the pair-correlation (PC) effects, coming through the $\bar{O}S_{1v}$+c.c. terms [10], are small. The role played by the different physical effects is evident from this figure. The overall trends exhibited by A for the $^{2}D_{5/2}$ states of the alkaline-earth-metal ions are indeed very peculiar compared to the single d-valence neutral atoms [11], and also single s and p valence atomic

TABLE VI. Contributions from different coupled-cluster terms to the magnetic dipole hyperfine structure constant (A) in MHz.

	^{9}Be^{+} (3d $^{2}D_{5/2}$)	^{25}Mg^{+} (3d $^{2}D_{5/2}$)	^{43}Ca^{+} (3d $^{2}D_{5/2}$)	^{87}Sr^{+} (4d $^{2}D_{5/2}$)	^{137}Ba^{+} (5d $^{2}D_{5/2}$)
Dirac-Fock (O)	−1.021	−0.539	−14.163	−13.006	51.612
$\bar{O}$	−1.021	−0.541	−14.448	−13.499	53.213
$\bar{O}S_{1v}$+c.c.	−0.006	−0.031	−3.438	−2.229	8.684
$\bar{O}S_{2v}$+c.c.	0.057	0.659	15.793	18.795	−78.272
$S_{1v}^{\dagger}\bar{O}S_{1v}$	$\sim$−0.000	−0.001	−0.226	−0.095	0.361
$S_{1v}^{\dagger}\bar{O}S_{2v}$	0.001	0.027	0.926	0.816	−3.107
$S_{2v}^{\dagger}\bar{O}S_{2v}$	−0.007	−0.007	−2.098	−1.678	7.424
Others	-7×10^{-7}	−0.002	−0.065	−0.044	−0.255
$\mathcal{N}$	$\sim$0.000	$\sim$−0.000	−0.075	−0.035	0.235

TABLE VIII. Contributions from different coupled-cluster terms to the ratio of the electric quadrupole hyperfine structure constants with their quadrupole moments (B/Q) in MHz/b^{-1}.

	^{9}Be$^+$ (3d $^2D_{5/2}$)	^{25}Mg$^+$ (3d $^2D_{5/2}$)	^{43}Ca$^+$ (3d $^2D_{5/2}$)	^{87}Sr$^+$ (4d $^2D_{5/2}$)	^{137}Ba$^+$ (5d $^2D_{5/2}$)
Dirac-Fock (O)	2.667	3.233	77.241	110.231	171.409
$\bar{O}$	2.667	3.246	77.072	117.983	181.948
$\bar{O}S_{1v}$+c.c.	0.017	0.185	18.295	18.697	31.179
$\bar{O}S_{2v}$+c.c.	−0.445	5.357	0.836	27.881	48.808
$S_{1v}^\dagger \bar{O} S_{1v}$	∼0.000	0.004	1.189	0.771	1.375
$S_{1v}^\dagger \bar{O} S_{2v}$	−0.001	0.051	−1.149	0.303	1.242
$S_{2v}^\dagger \bar{O} S_{2v}$	0.013	−0.168	0.541	−1.424	−4.584
Others	-2×10^{-6}	0.002	−0.359	−0.031	47.563
$\mathcal{N}$	∼−0.000	−0.006	−2.726	−2.505	−4.931

systems [10,12]. This peculiarity can undoubtedly be attributed to the overwhelming contributions of the CP effects to the magnetic dipole hyperfine constants of the states that we have investigated.

We also present the calculated B results in Table VII and compare with other calculated results using various theories along with their experimental results. As seen from this table, our results are very close with the experimental results and therefore it highlights the fact that the RCC method is powerful than other used many-body theories employed to calculate these quantities. To understand the behavior of electron correlation effects arising through various physical effects in these calculations, we present individual contributions from different RCC terms to B in Table VIII. It shows that the final results have the same sign as the DF results in contrast to results for A of the corresponding states. From Tables VI and VII, it is obvious that the PC and CP effects also have the same signs, but the CP effects are small compared to the PC effects for the light systems while they are large in Sr$^+$ and Ba$^+$.

Our results are considerable improvements over those of previous calculations, which were performed by different variants of many-body perturbation theories except the latest that is based on the relativistic configuration interaction (RCI) method [35]. The RCI calculations by Itano use a multiconfiguration DF extended optimized level (MCDF-EOL) single particle basis. He considers only a subset of the single and double excitations used in our calculations, and the core excitations are limited only to a few outer core electrons. Also, he has excluded the nonlinear terms present in our

RCC wave functions given in Eq. (2.4). For Sr$^+$ and Ba$^+$, the RCI calculations give wrong signs for A (see Table V), thereby highlighting the extraordinarily strong correlation effects in these two systems. The relativistic many body-perturbation theory calculation of Yu *et al.* for Sr$^+$ [34] has been carried out to second order in contrast to our all-order calculation. Martesnsson-Pendrill's partial RCC calculation [36] is in poor agreement with experiment as it is unable to cope with the sensitive pair correlation effects that influence the hyperfine interaction constant for the $^2D_{5/2}$ state of Sr$^+$.

V. CONCLUSION

Our present work on the hyperfine structure constants of the $^2D_{5/2}$ states of the alkaline-earth-metal ions is a testament to the remarkable ability of the relativistic coupled-cluster theory to successfully capture very strong correlation effects even when other widely used methods such as the finite order relativistic many-body perturbation theory, and the relativistic configuration interaction fail. This feature, if suitably exploited, can yield a wealth of very useful information about a wide range of the atomic properties.

[1] C. Champenois, M. Houssin, C. Lisowski, M. Knoop, G. Hagel, M. Vedel, and F. Vedel, Phys. Lett. A **331**, 298 (2004).

[2] G. P. Barwood, G. Huang, H. A. Klein, P. Gill, and R. B. M. Clarke, Phys. Rev. A **59**, R3178 (1999).

[3] J. A. Sherman, W. Trimble, S. Metz, W. Nagourney, and N. Fortson, eprint arXiv:physics/0504013.

[4] C. F. Roos, M. Riebe, H. Häffner, W. Hänsel, J. Benhelm, G. P. T. Lancastar, C. Becher, F. Schmidt-Kaler, and R. Blatt, Science **304**, 1478 (2004).

[5] K. P. Geetha, A. D. Singh, B. P. Das, and C. S. Unnikrishnan, Phys. Rev. A **58**, R16 (1998).

[6] P. Beiersdorfer, C. M. Lisse, R. E. Olson, G. V. Brown, and H.

P. Chen, Astrophys. J. **549**, L147 (2001).

[7] W. M. Itano, J. Res. Natl. Inst. Stand. Technol. **105**, 829 (2000).

[8] I. Lindgen and J. Morrison, *Atomic Many-Body Theory*, edited by G. Ecker, P. Lambropoulos, and H. Walther (Springer-Verlag, Berlin, 1985).

[9] B. K. Sahoo, S. Majumder, R. K. Chaudhuri, B. P. Das, D. Mukherjee, J. Phys. B **37**, 3409 (2004).

[10] B. K. Sahoo, G. Gopakumar, R. K. Chaudhuri, B. P. Das, H. Merlitz, U. S. Mahapatra, and D. Mukherjee, Phys. Rev. A **68**, 040501(R) (2003), and references therein.

[11] B. K. Sahoo, T. Beier, B. P. Das, R. K. Chaudhuri, and D. Mukherjee, J. Phys. B **39**, 355 (2006).

[12] B. K. Sahoo, R. K. Chaudhuri, B. P. Das, H. Merlitz, and D. Mukherjee, Phys. Rev. A **72**, 032507 (2005).

[13] G. Gopakumar, H. Merlitz, S. Majumder, R. K. Chaudhuri, B. P. Das, U. S. Mahapatra, and D. Mukherjee, Phys. Rev. A **64**, 032502 (2001).

[14] B. K. Sahoo, R. K. Chaudhuri, B. P. Das, and D. Mukherjee, Phys. Rev. Lett. **96**, 163003 (2006).

[15] G. Gopakumar, H. Merlitz, R. K. Chaudhuri, B. P. Das, U. S. Mahapatra, and D. Mukherjee, Phys. Rev. A **66**, 032505 (2002).

[16] B. K. Sahoo, Sonjoy Majumder, H. Merlitz, R. K. Chaudhuri, B. P. Das, and D. Mukherjee, J. Phys. B **39**, 355 (2006).

[17] B. K. Sahoo, R. K. Chaudhuri, B. P. Das, and D. Mukherjee, Phys. Rev. Lett. **96**, 163003 (2006).

[18] C. Sur, K. V. P. Latha, B. K. Sahoo, R. K. Chaudhuri, B. P. Das, and Debashis Mukherjee, Phys. Rev. Lett. **96**, 193001 (2006).

[19] C. Schwartz, Phys. Rev. **97**, 380 (1955).

[20] K. T. Cheng and W. J. Childs, Phys. Rev. A **31**, 2775 (1985).

[21] D. Mukherjee and S. Pal, Adv. Quantum Chem. **20**, 281 (1989).

[22] R. K. Chaudhuri, P. K. Panda, and B. P. Das, Phys. Rev. A **59**, 1187 (1999).

[23] F. A. Parpia and A. K. Mohanty, Phys. Rev. A **46**, 3735 (1992).

[24] For example see, P. Raghavan, At. Data Nucl. Data Tables **42**, 189 (1989).

[25] B. K. Sahoo, Phys. Rev. A **73**, 062501 (2006).

[26] W. Norterhauser, K. Blaum, K. Icker, P. Muller, A. Schmitt, K. Wendt, and B. Wiche, Z. Phys. D: At., Mol. Clusters **2**, 33 (1988).

[27] G. P. Barwood, K. Gao, P. Gill, G. Huang, and H. A. Klein, Phys. Rev. A **67**, 013402 (2003).

[28] J. Huennekens and A. Gallagher, Phys. Rev. A **27**, 1851 (1983).

[29] R. E. Silverans, G. Borghs, G. Dumont, and J.-M. Van den Cruyce, Z. Phys. A **295**, 311 (1980).

[30] R. E. Silverans, G. Borghs, P. De Bisschop, and M. Van Hove, Phys. Rev. A **33**, 2117 (1986).

[31] M. S. Safronova, A. Derevianko, and W. R. Johnson, Phys. Rev. A **58**, 1016 (1998).

[32] A.-M. Mårtensson-Pendrill and S. Salomonson, Phys. Rev. A **30**, 712 (1984).

[33] A.-M. Mårtensson-Pendrill, A. Ynnerman, H. Warston, L. Vermeeren, R. E. Silverans, A. Klein, R. Neugart, C. Schulz, P. Lievens, and The ISOLDE Collaboration, Phys. Rev. A **45**, 4675 (1992).

[34] K. Z. Yu, L. J. Wu, B. C. Gou, and T. Y. Shi, Phys. Rev. A **70**, 012506 (2004).

[35] W. M. Itano, Phys. Rev. A **73**, 022510 (2006).

[36] A.-M. Maartensson-Pendrill, J. Phys. B **35**, 917 (2002).

[37] W. Nortershauer, K. Blaum, K. Icker, P. Muller, A. Schmitt, K. Wendt, and B. Wiche, Z. Phys. D: At., Mol. Clusters **2**, 33 (1988).